Chapter 6

Successful Application of the CCM to the Rabi Hamiltonian

In order to determine whether quantitatively accurate results for the Rabi Hamiltonian can be obtained using a CCM calculation which takes into account the symmetries of the Hamiltonian, we investigate the use of various coupling–dependent CCM model states for the Rabi Hamiltonian, as well as the application of the method to a unitary transformed Hamiltonian.

6.1 Coupling–dependent CCM model states for the Rabi Hamiltonian

It is significant that, like TIPT, the CCM based on the noninteracting model state of Schemes I and II breaks down in the transitional region where the Rabi ground state undergoes the marked change in character discussed in Section 4.2. This suggests that the noninteracting model state should be replaced by a coupling–dependent model state capable of following this character change. For Scheme III, we therefore perform an NCCM calculation based on a model state of the form $|\Phi\rangle = |\Psi_+\rangle$ [see (4.16)], which is a coupling–dependent, even–parity superposition of the coherent states (4.11), and which we shall thus refer to as the coherent superposition (CS) model state (see Table D.1). The CS model state is an exact eigenstate of $H_{\rm Rabi}$ not only in the $\omega_0 = 0$ ($g \to \infty$) limit, but also in the $g = 0$ limit, where it reduces to the noninteracting model state. The correlation operator

$$S = \sum_{n=1}^{\infty} s_n \left(c^\dagger\right)^n , \qquad c^\dagger \equiv b^\dagger \sigma^x + \frac{2g}{\omega} \tag{6.1}$$

for Scheme III again incorporates the required even–parity symmetry in the CCM ground state. Note that the CCM creation operators $\left\{\left(c^\dagger\right)^n\right\}$ have been chosen so as to satisfy the requirement that the set $\left\{\left(c^\dagger\right)^n |\Phi\rangle\right\}$ is complete, and also so that their Hermitian conjugates $\{c^n\}$ conveniently annihilate the CS model state. As for Scheme II, the nested commutator expansion (3.8), rather than terminating, assumes a closed form (see Equation (D.21) in Appendix D), and one obtains for the ground–state energy

$$E_0^{\rm NCCM,III} = -\frac{1}{2}\,\omega_0\, e^{-8g^2/\omega^2}\, \exp\left\{\sum_{n=1}^{\infty} s_n \left(\frac{4g}{\omega}\right)^n\right\} - \frac{4g^2}{\omega} . \tag{6.2}$$

We have used *Mathematica* [Mat] to set up the energy functional $\overline{H}$ and the CCM equations (3.14) for the coefficients $\{s_n\}$ and $\{\tilde{s}_n\}$ (see Equations (D.23) and (D.25) in Appendix D).

In Table 6.1 we tabulate the resonant Scheme III ground–state energy results, which are indistinguishable from the CI results on the scale of our

Table 6.1: *The ground–state energy of the scaled resonant ($\omega = \omega_0 = 1$) Rabi Hamiltonian as a function of the coupling g as determined via a SUB-10 NCCM Scheme III calculation, labelled $E_0^{\mathrm{NCCM,III}}$, and via a SUB-10 NCCM analysis based on Scheme IV, labeled $E_0^{\mathrm{NCCM,IV}}$ (see Table D.1). For comparison, we also tabulate results obtained via a CI diagonalization in a basis of 101 even–parity states, labelled E_0^{CI}, as well as the results of the benchmark three–parameter variational calculation, labelled E_0^{PBV3}.*

g	E_0^{CI}	$E_0^{\mathrm{NCCM,IV}}$	$E_0^{\mathrm{NCCM,III}}$	E_0^{PBV3}
0.0	-0.50000	-0.50000	-0.50000	-0.50000
0.1	-0.52020	-0.52020	-0.52020	-0.52020
0.2	-0.58333	-0.58333	-0.58333	-0.58333
0.3	-0.69762	-0.69762	-0.69763	-0.69757
0.4	-0.87855	-0.87847	-0.87882	-0.87822
0.5	-1.14795	-1.14642	-1.14964	-1.14676
0.6	-1.52396	-1.51961	-1.52343	-1.52211
0.7	-2.00825	-2.00414	-1.99657	-2.00685
0.8	-2.59070	-2.58827	-2.57057	-2.58998
0.9	-3.26191	-3.26061	-3.24192	-3.26158
1.0	-4.01693	-4.01620	-4.00028	-4.01677

figures, as a function of g, along with the benchmark three–parameter variational ground–state energy results. To moderate order (SUB-10), the results show good agreement, over the full coupling spectrum, with the results of the CI diagonalization. Some comments are however in order: To higher order ($\sim$ SUB-20 and above), we find that the NCCM Scheme III solution breaks down in isolated coupling regions, possibly for numerical reasons. Furthermore, for Scheme III, the NCCM result for $\langle \sigma_z \rangle$ (which is shown in Figure 6.1 along with the Scheme I results for comparison; explicit expressions for $\langle \sigma_z \rangle$ in both schemes are given in Equations (D.5) and (D.27) in Appendix D) also fails quantitatively in and above the transitional region, even in moderate order (SUB-10) where the CCM ground–state energy is in very good agreement with the CI result. In this regard, it is significant that the Scheme III analysis fails to resolve the (admittedly small) difference between the exact ground–state energy and the so–called baseline energy $-4g^2/\omega$ for $g \sim 1$. Thus the CS model state of Scheme III, though a definite improvement on the noninteracting model state, is still not entirely capable of tracking the character change in the Rabi ground state.

We have therefore also performed an NCCM calculation based on a coupling–dependent model state of the even–parity two–parameter variational form (4.38) (see Scheme IV in Table D.1), which also reduces to the exact ground state in both the limits of small and infinitely large coupling. For Scheme IV, we use the same (even–parity) correlation operator S as for Scheme II. This computationally convenient choice has some drawbacks: The set of states $\{\left(c^\dagger\right)^n |\Phi\rangle\}$; $n = 0, 1, 2, \ldots$ does not span the many–body Hilbert space, and the Hermitian–adjoint destruction operators $\{c^n\}$, $n \geq 1$ do not annihilate

Figure 6.1: *The expectation value of σ_z in the ground state of the scaled resonant ($\omega = \omega_0 = 1$) Rabi Hamiltonian as a function of the coupling g as determined via a SUB-N, N=10,50, NCCM analysis based on Scheme I (thin solid lines), as well as via a SUB-10 NCCM analysis based on Scheme III (dotted line), compared to results obtained via a CI diagonalization (solid line) in a basis of 101 even-parity states.*

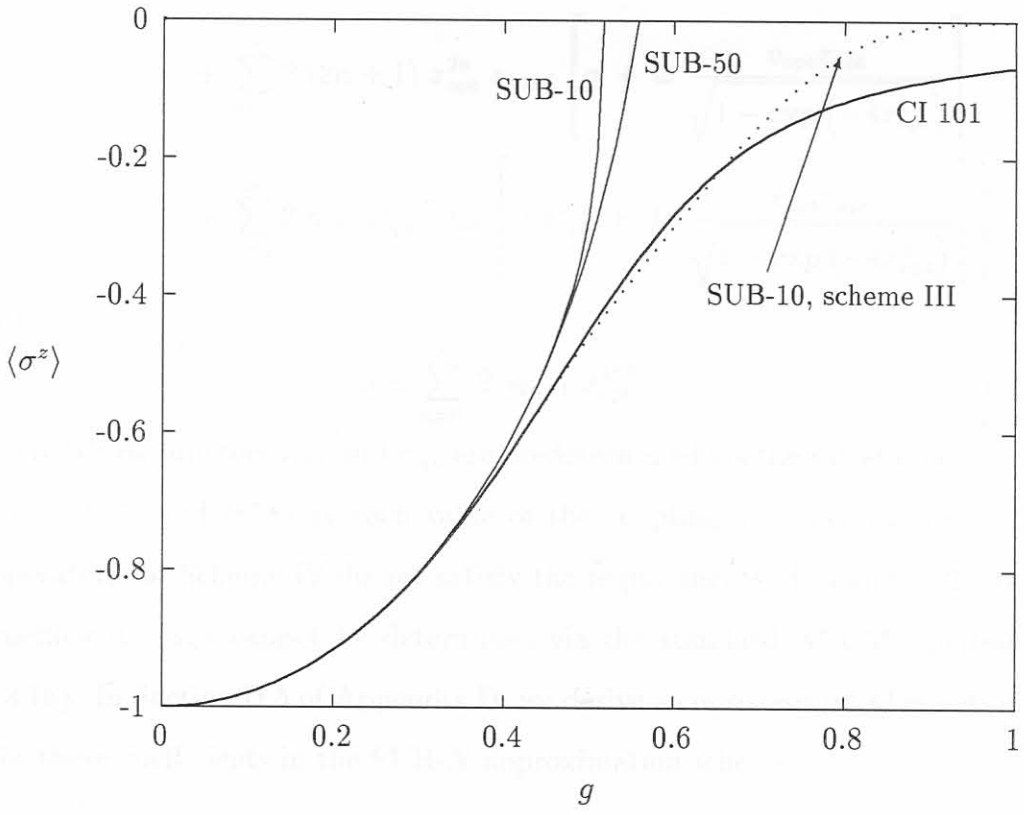

the model state. The purpose of this calculation, however, is simply to show that the CCM may be successfully applied to the Rabi Hamiltonian *provided* that a suitable model state is chosen. As for Schemes II and III, the nested commutator expansion (3.8) assumes a closed form (see Equation (D.28) in

Appendix D), and we obtain for the ground–state energy in Scheme IV

$$
\begin{aligned}
E_0^{\mathrm{NCCM,IV}} \;=\; & \frac{1}{\sqrt{1+v_{\mathrm{opt}}^2}} \Bigg\{ \frac{1}{2}\,\omega_0\,\cosh\alpha\,\left(v_{\mathrm{opt}}^2-1\right) \\
& + \omega_0\,\sinh\alpha\,\frac{v_{\mathrm{opt}}\exp\left(-2x_{\mathrm{opt}}^2\right)}{\sqrt{1-\exp\left(-4x_{\mathrm{opt}}^2\right)}} \\
& + 8\,g\,\frac{v_{\mathrm{opt}}x_{\mathrm{opt}}}{\sqrt{1-\exp\left(-4x_{\mathrm{opt}}^2\right)}} \;+\; \omega\,x_{\mathrm{opt}}^2\,\left(\tanh x_{\mathrm{opt}}^2 + v_{\mathrm{opt}}^2\coth x_{\mathrm{opt}}^2\right) \\
& + \sum_{n=0}^{\infty} 2\,(2n+1)\,x_{\mathrm{opt}}^{2n}\,s_{2n+1}\left[g \;+\; \omega\,\frac{v_{\mathrm{opt}}x_{\mathrm{opt}}}{\sqrt{1-\exp\left(-4x_{\mathrm{opt}}^2\right)}}\right] \\
& + \sum_{n=1}^{\infty} 2\,n\,\omega\,x_{\mathrm{opt}}^{2n-2}\,s_{2n}\left[\omega\,x_{\mathrm{opt}}^2 \;+\; 4g\,\frac{v_{\mathrm{opt}}x_{\mathrm{opt}}}{\sqrt{1-\exp\left(-4x_{\mathrm{opt}}^2\right)}}\right]\Bigg\}, \qquad (6.3)
\end{aligned}
$$

with

$$
\alpha \equiv \sum_{n=0}^{\infty} 2\,s_{2n+1}\,x_{\mathrm{opt}}^{2n+1}\,. \qquad (6.4)
$$

Here the parameters x_{opt} and v_{opt} are predetermined via the variational equations (C.7) and (C.8) at each value of the coupling g. Since the creation operators for Scheme IV do not satisfy the requirements (3.1) and (3.2), the coefficients $\{s_n\}$ cannot be determined via the standard NCCM equations (3.16). In Section D.5 of Appendix D, we derive a consistent set of equations for these coefficients in the SUB-N approximation scheme.

It is clear from ground–state energy results shown in Table 6.1 that the NCCM based on Scheme IV yields excellent agreement with the CI diagonalization for all couplings. Thus it is possible to obtain very good CCM ground–state energy results for the Rabi Hamiltonian, provided that a coupling–dependent model state is chosen which, besides the parity symmetry, also incorporates the important physical features of the exact ground

state, in particular the change in character in the transitional region. It is also straightforward to adapt the NCCM Scheme III and IV approaches above in order to determine the odd–parity first excited state energy E_1 via the CCM (see Table D.2 in Appendix D). In Table 6.2 we tabulate the NCCM Scheme IV results for E_1, which are again in very good agreement with the CI results. Note, however, that when considered over the full coupling spectrum, the three–parameter variational calculation outperforms even the Scheme IV

Table 6.2: *The first excited state energy of the scaled resonant ($\omega = \omega_0 = 1$) Rabi Hamiltonian as a function of the coupling g as determined via a SUB-10 NCCM Scheme IV calculation, labelled $E_1^{\mathrm{NCCM,IV}}$, compared to results obtained via a CI diagonalization in a basis of 101 odd–parity states, labelled E_1^{CI}, and via the benchmark three–parameter variational calculation, labelled E_1^{PBV3}.*

g	E_1^{CI}	$E_1^{\mathrm{NCCM,IV}}$	E_1^{PBV3}
0.0	0.50000	0.50000	0.50000
0.1	0.28067	0.28064	0.28074
0.2	0.02337	0.02328	0.02396
0.3	-0.27391	-0.27386	-0.27237
0.4	-0.61609	-0.61555	-0.61376
0.5	-1.01018	-1.00895	-1.00774
0.6	-1.46444	-1.46268	-1.46256
0.7	-1.98701	-1.98518	-1.98587
0.8	-2.58432	-2.58283	-2.58373
0.9	-3.26028	-3.25924	-3.25999
1.0	-4.01658	-4.01590	-4.01643

NCCM calculation at a fraction of the computational cost.

Due to the fact that the creation operators and model state of Scheme IV do not satisfy the requirements (3.1) and (3.2), it is difficult to set up a consistent set of equations for the NCCM bra state coefficients $\{\tilde{s}_n\}$. We have therefore not calculated the expectation value of observables other than the Hamiltonian in the NCCM Scheme IV ground state. However, given the ground and first excited state energy results presented above, we do not expect that the CCM would yield more accurate results for quantities such as σ^z than those obtained via the even–parity three–parameter variational calculation.

6.2 The method of unitary transformations

The method of unitary transformations offers an alternative approach to the application of the CCM to the Rabi Hamiltonian. In this approach, a unitary rotation $U = \exp R$, $R^\dagger = -R$ is applied to the Hamiltonian, leaving the spectrum unchanged, and the CCM is then applied to the transformed Hamiltonian $H^U = U^\dagger H U$. In their analysis of the multimode Rabi system, Wong and Lo [Wo96b] applied a unitary displacement transformation of the form

$$U_1 = \exp R_1, \quad R_1 = \frac{2g}{\omega}\left(b^\dagger - b\right) , \tag{6.5}$$

to the Hamiltonian. We have performed an NCCM calculation, based on the model state and creation operators of Scheme I, for the transformed Rabi Hamiltonian $H^{U_1}_{\text{Rabi}}$. Since the transformation (6.5) does not conserve the

parity Π_{rabi}, this NCCM calculation is not restricted to the even–parity sector as before, and it is no longer possible within the CCM to distinguish between the ground and first excited states on the basis of their parity symmetry. Due to the disregard for the parity symmetry, the CCM ground–state energy results are quantitatively inaccurate in and above the transitional region (as is the case for the multimode Rabi system considered in [Wo96b]). Futhermore, since the results are considerably less accurate than those obtained via, say, the even–parity two–parameter variational calculation, these results are not presented here.

We have also considered the application of the CCM to the transformed Hamiltonian $H_{\text{Rabi}}^{U_2}$, where U_2 represents a more general unitary rotation of the form

$$U_2 = \exp R_2, \quad R_2 = \beta\left(b^\dagger - b\right) + i\gamma\sigma^y \,. \tag{6.6}$$

However, since the transformation (6.6) does not conserve parity, the same comments apply as for (6.5). The NCCM ground–state energy results (not shown here) are in excellent agreement with the diagonalization results for large coupling ($g \geq 0.7$), and are comparable to the results obtained via the three–parameter variational calculation in this region. The CCM solution, however, terminates upon entering the transitional region from above, and is therefore not shown here.

Thus, despite moderate success, neither of the above CCM calculations based a unitary transformed Rabi Hamiltonian yield good results over the full coupling spectrum. This is at least partly due to the fact that both rotations destroy the parity symmetry Π_{Rabi}. One may also consider a parity–

conserving unitary transformation of the Rabi Hamiltonian of the form

$$U_3 = \exp R_3, \quad R_3 = \frac{2g}{\omega}\left(b - b^\dagger\right)\sigma^x \,. \tag{6.7}$$

The algebra involved in an NCCM analysis of the rotated Hamiltonian $H_{\rm Rabi}^{U_3}$ becomes prohibitively involved beyond the level of the SUB-1 approximation. Note however that, since the CS model state $|\Psi_+\rangle$ of Scheme III may be written in the form

$$|\Psi_+\rangle = e^{-x^2/2}\exp R_3|0\rangle|\downarrow\rangle \,, \tag{6.8}$$

it is clear that a SUB-1 NCCM Scheme I calculation on the rotated Hamiltonian $H_{\rm Rabi}^{U_3}$ is equivalent to a SUB-1 NCCM Scheme III calculation on the unrotated Rabi Hamiltonian (4.1). Although this is no longer true in the SUB-N, $N \geq 2$ approximation, we do not expect the results of this calculation to differ qualitatively from those obtained via our NCCM Scheme III analysis of the unrotated Rabi Hamiltonian.